Parallel Synthesis and Study of Fluorous Biphasic Partition Coefficients of 1*H*,1*H*,2*H*,2*H*-Perfluoroalkylsilyl Derivatives of Triphenylphosphine: A Statistical Approach

Elwin de Wolf,[†] Eva Riccomagno,[‡] Jeroen J. M. de Pater,[†] Berth-Jan Deelman,*,[§] and Gerard van Koten[†]

Debye Institute, Department of Metal-Mediated Synthesis, Utrecht University, Padualaan 8, NL-3584 CH Utrecht, The Netherlands, Department of Statistics, University of Warwick, CV4 7AL Coventry, United Kingdom, and ATOFINA Vlissingen B.V., P.O. Box 70, NL-4380 AB Vlissingen, The Netherlands

A library of fluorous, (1*H*,1*H*,2*H*,2*H*-perfluoroalkyl)silyl-substituted derivatives of triphenylphosphine, $Ph_{3-a}P[C_6H_{5-y}\{SiMe_{3-b}(CH_2CH_2C_xF_{2x+1})_b\}_y\text{-}pos]_a$ [$a = 1-3$; $b = 1-3$; $x = 4, 6, 8$, or 10; $pos = 3, 4$ ($y = 1$) or $3,5$ ($y = 2$)], was prepared using parallel synthetic techniques. Upon variation of these four parameters, a total of 108 different fluorous phosphines can be synthesized. Using factorial design, 37 phosphines were selected and their partition coefficients in the typical fluorous biphasic solvent system PFMCH/toluene (PFMCH = perfluoromethylcyclohexane) determined. By fitting of the partition coefficient data to linear functions of the parameters *a*, *b*, and *x*, the partition coefficients of the remaining 71 fluorous phosphines, which were not prepared, could be predicted. Using this approach, some unexpected trends in the dependence of the partition coefficient on variations of the four parameters became clear, resulting in a better understanding of the optimum fluorous substitution pattern for obtaining the highest partition coefficient (*P*). In this way, the partition coefficient was increased by 2 orders of magnitude, i.e., from the initial value $P = 7.8$ for **1**(3, 2, 6, C4) to $P > 238$ for **1**(2, 3, 6, C3C5). Para- and 3,5-substituted phosphines showed irregular behavior in the sense that elongation or increase of the number of perfluoroalkyl tails did not necessarily lead to higher partition coefficients. Particularly high values were found for phosphines containing a total of 72 fluorinated carbon atoms on the meta position(s) of the aryl rings. Linear relationships were found between the predicted log *P* of **1**(*a*, *b*, *x*, C4) and the experimentally determined log *P* values of fluorous diphosphines $[CH_2\{C_6H_4(SiMe_{3-b}(CH_2CH_2C_6F_{13})_b)\text{-}4\}_2]_2$ and monophosphines $Ph_{3-a}P\{C_6H_4(CH_2CH_2C_6F_{13})\text{-}4\}_a$. One of the most fluorophilic phosphines, i.e., **1**(3, 1, 8, C3C5), was applied and efficiently recycled in rhodium-catalyzed, fluorous hydrosilylation of 1-hexene by $HSiMe_2Ph$ using PFMCH as the fluorous phase and the substrates as the organic phase. It was demonstrated that a higher partition coefficient of the ligand in PFMCH/toluene at 0 °C indeed resulted in less leaching of both the catalyst and the free ligand during phase separation.

Introduction

Fluorous biphasic catalyst separation has become a well-demonstrated technique for catalyst recycling in several homogeneously catalyzed processes.[1] Among all ligands of which a fluorous analogue is now available, trialkyl- and triarylphosphines are probably the best known.[1,2] Although numerous fluorous phosphines have been reported in the literature and applied in fluorous-phase catalysis,[3,4] only a few quantitative studies have been performed. Hence, the relationship between the partition coefficient (*P*) and the molecular structure of the phosphine remains poorly understood ($P = c_{\text{fluorous phase}}/c_{\text{organic phase}}$). Some general trends can be observed, however. For example, elongation of the perfluoroalkyl tail often, but not always, results in higher

partition coefficients. Furthermore, fluorous alkylphosphines exhibit better partitioning in favor of the fluorous phase than fluorous arylphosphines, e.g., $P > 332$ for $P(CH_2CH_2C_8F_{17})_3$ and $P = 2.0$ for $P[C_6H_4\{(CH_2)_3C_8F_{17}\}\text{-}4]_3$ in *c*-$C_6F_{11}CF_3$ (PFMCH)/toluene at room temperature. Because there is a direct relationship between the partition coefficient of the fluorous phosphine ligand and the leaching of the catalyst in fluorous biphasic catalyst recycling,[5] a systematic study of the factors that control the partition coefficient is needed for efficient ligand design that minimizes catalyst leaching. Several papers that help to gain a better thermodynamic understanding of the relationship between the partition coefficients of relatively small fluorous organic molecules and their structural characteristics were recently published.[6] Even a more universal theory that correctly predicts the log *P* values of fluorous compounds on the basis of their molar volumes and nonspecific cohesion parameters has been developed.[7] However, these models cannot be transferred

* To whom correspondence should be addressed. Fax: +31 113 612984. E-mail: berth-jan.deelman@atofina.com.
† Utrecht University.
‡ University of Warwick.
§ ATOFINA Vlissingen B.V.

directly to new subsets of molecules for which the model was not specifically trained and do not correctly predict the effects of specific structural variations within closely related or isomeric sets of molecules.

Previously, we published a report on *para*-silyl-substituted fluorous derivatives of triphenylphosphine, $P[C_6H_4\{SiMe_{3-b}-(CH_2CH_2C_xF_{2x+1})_b\}-p]_3$ ($b = 1-3$; $x = 6, 8$)[8] and their application in fluorous hydrogenation[5] and hydrosilylation.[9] Their partition coefficients in several fluorous biphasic solvent systems were investigated, and surprisingly, maximum values were found only at relatively low weight percentages of fluorine ($P = 7.8$ at $b = 2$ and $x = 6$ in PFMCH/toluene at 0 °C). A further increase of the weight percentage of fluorine resulted in a decrease of P. To obtain phosphines with even higher partition coefficients with a minimum of synthetic effort, we decided to use statistical techniques for the prediction of the partition coefficients of a library of silyl-substituted fluorous derivatives of triphenylphosphine (**1**). Combinatorial synthetic techniques were used to prepare a basis set of library members. The log P values of the individual library members were determined and served as experimental input for fitting of the statistical models.

Results and Discussion

Each member of the library can be uniquely described by four parameters: a, b, x, and *pos* (see structures of **1**), where a is the number of silyl-substituted phenyl groups ($a = 1-3$), b is the number of tails attached per silicon atom ($b = 1-3$), x denotes the length of the perfluoroalkyl group ($x = 4, 6, 8, 10$), and *pos* refers to the positions at the aryl ring (*pos* = C3, C4, or C3C5) that are silylated.
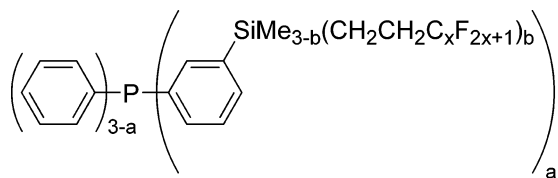
1(*a*, *b*, *x*, C3)
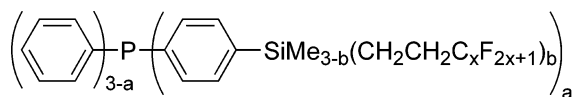
1(*a*, *b*, *x*, C4)
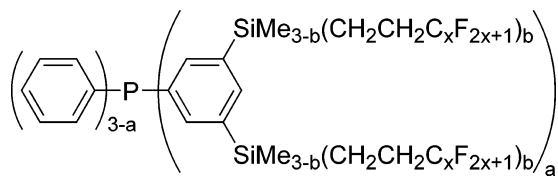
1(*a*, *b*, *x*, C3C5)

$a = 1-3$
$b = 1-3$
$x = 4, 6, 8$ or 10

The total number of tails per phosphine is then given by *ab* (*pos* = C3, C4) or 2*ab* (*pos* = C3C5), and the total number

of fluorinated carbon atoms is given by *abx* (C3, C4) and 2*abx* (C3C5). No tails longer than $C_{10}F_{21}$ were used because of commercial unavailability and synthetic reasons. If the boiling points of the starting compounds become too high, purification becomes difficult. Similarly, no tails shorter than C_4F_9 were used to avoid gaseous reactants. To reduce the total number of 108 ligands to be synthesized, statistical methods, in particular experimental design, were used to select a portion of the total 4D-parameter space and gain information on unselected phosphines. In this way, time could be saved as well as costs, as lower amounts of starting materials and reagents were needed.

Selection of Compounds to Synthesize. The fluorous phosphines **1**(*a*, *b*, *x*, *pos*) were synthesized and their partition coefficients analyzed in four blocks of 7−13 compounds. The phosphines in each block are listed in Table 1. An iterative approach based on statistical stepwise regression was followed, i.e., the results of the previous blocks were used for the selection of the phosphines to synthesize in the next block (for more details, see the Experimental Section). In this way, the selection of phosphines that were to be prepared could be done quickly, resulting in optimal partition coefficients in the chosen PFMCH/toluene (1:1, v/v) system (vide infra), while inference on the whole design was still possible, i.e., knowledge about the influence of *a*, *b*, *x*, and *pos* on the partition coefficient.

**Parallel Synthesis.** The starting fluorous halosilanes [**3**(*b*, *x*)][8−10] and brominated derivatives of triphenylphosphine [**4**(*a*, *pos*)][11] were synthesized according to published procedures (Schemes 1 and 2). Some fluorous silanes, notably **2**(*b*, *x*) and **3**(*b*, *x*) ($b = 2$, $x = 4, 6, 8, 10$; $b = 3$; $x = 4$) contained small amounts of Wurtz-coupling products [$(C_xF_{2x+1}-CH_2CH_2)_2$], which were difficult to remove, by either washing or (Kugelrohr) distillation. Therefore, these silanes were used without further purification.[12] The side products were easily removed once the fluorous triphenylphosphine was formed.

All fluorous phosphines **1**(*a*, *b*, *x*, *pos*), except the previously reported **1**(3, *b*, *x*, C4) ($b = 1-3$; $x = 6, 8$)[8] and the 3,5-substituted phosphines **1**(*a*, *b*, *x*, C3C5), were prepared in parallel from **3**(*b*, *x*) and **4**(*a*, *pos*) in series of 10 compounds at a time and on 50−200-mg scale (Scheme 3). An excess of *t*-BuLi (2.3*a* or 4.6*a* equiv for *pos* = C3 or C4 and C3C5, respectively) was added to favor complete lithiation. The relatively high reaction temperature (−40 °C) was dictated by the lower limit of the parallel synthesis equipment used. Compounds **1**(*a*, *b*, *x*, C3C5) were synthesized by conventional methods, because larger amounts of *t*-BuLi had to be added and the starting phosphines [**4**(*a*, C3C5)] dissolved only in THF, which required reaction temperatures lower than −40 °C.

All phosphines were purified by either aqueous workup or removal of volatiles in vacuo followed by extraction in a PFMCH/MeOH biphasic system. Compound **1**(3, 3, 10, C4) could not be obtained at sufficient purity because of its low solubility in all solvents. The purity of the 31 newly prepared phosphines was verified by ^{1}H NMR spectroscopy, by ^{31}P NMR spectroscopy, in some cases by ^{13}C and ^{19}F NMR-spectroscopies, and in 11 cases by elemental analysis. In

Table 1. Fluorous Phosphines **1**(*a, b, x, pos*) Synthesized in Different Blocks

first block	second block	third block	fourth block
1(3, 1, 6, C4)	**1**(1, 1, 8, C3)	**1**(2, 2, 6, C3)	**1**(2, 2, 4, C3C5)
1(3, 2, 6, C4)	**1**(1, 2, 8, C4)	**1**(2, 3, 6, C4)	**1**(2, 3, 6, C3C5)
1(3, 3, 6, C4)	**1**(2, 1, 8, C4)	**1**(2, 3, 8, C4)	**1**(2, 3, 8, C3C5)
1(3, 1, 8, C4)	**1**(2, 1, 10, C4)	**1**(3, 1, 10, C4)	**1**(3, 2, 6, C3C5)
1(3, 2, 8, C4)	**1**(2, 3, 4, C3)	**1**(3, 2, 4, C4)	**1**(3, 2, 8, C3C5)
1(3, 3, 8, C4)	**1**(2, 3, 6, C3)	**1**(3, 2, 4, C3)	**1**(3, 3, 4, C3C5)
1(3, 1, 6, C3)	**1**(2, 3, 8, C3)	**1**(3, 2, 8, C3)	**1**(3, 3, 10, C3C5)
1(3, 2, 6, C3)	**1**(3, 3, 4, C4)	**1**(3, 3, 8, C3)	
1(3, 3, 6, C3)		**1**(3, 3, 4, C3)	
		1(3, 1, 4, C3C5)	
		1(3, 1, 6, C3C5)	
		1(3, 1, 8, C3C5)	
		1(3, 1, 10, C3C5)	

Scheme 1
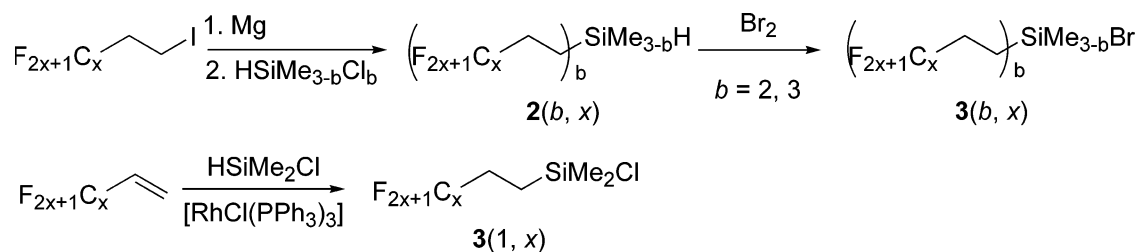
Scheme 2
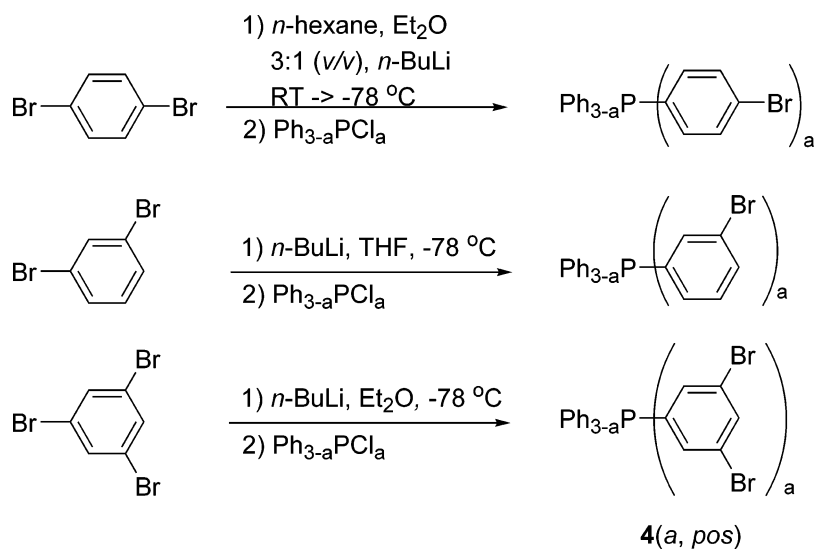
Scheme 3
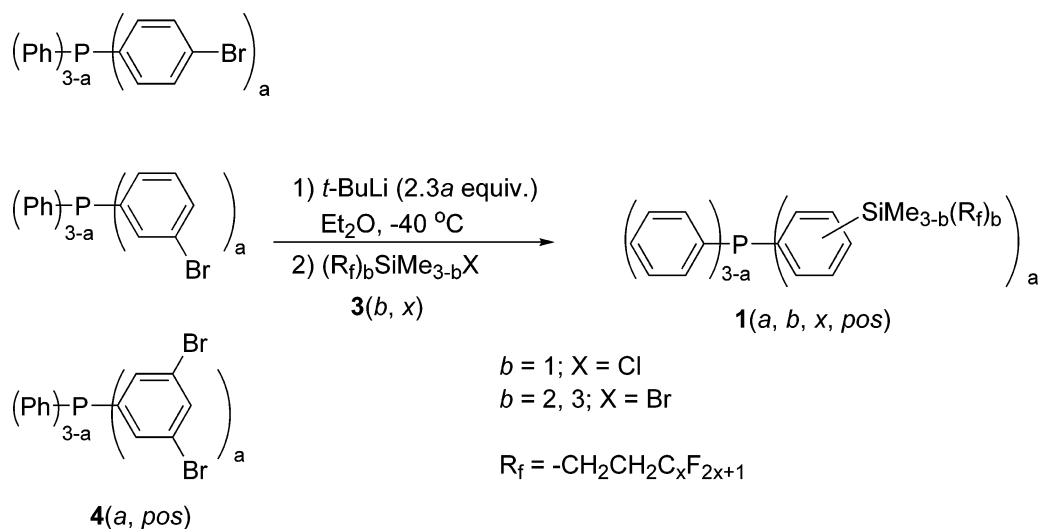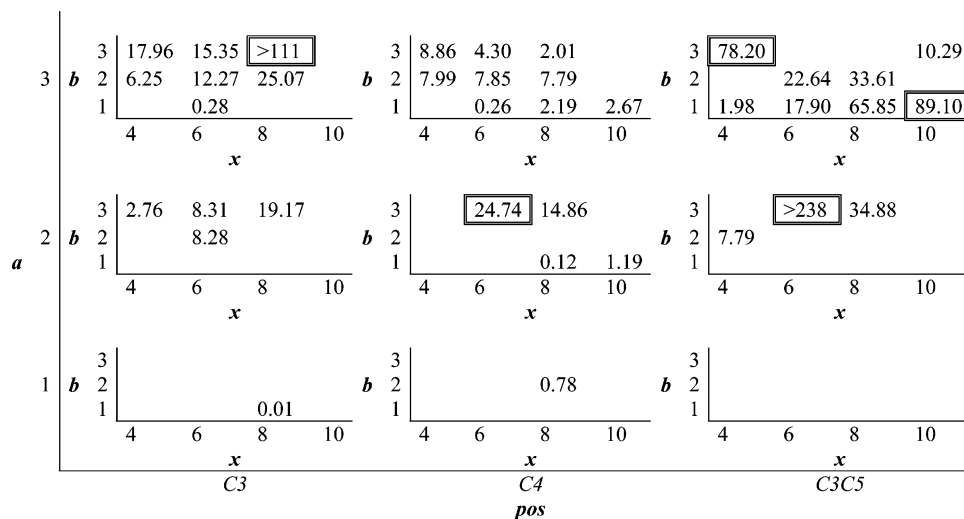
Figure 1. Partition coefficients of **1**(*a*, *b*, *x*, *pos*) in PFMCH/toluene at 0 °C.

general, the purities were found to be >95% (see also the Experimental Section and Table 7).

   Partition Coefficients of 1(*a*, *b*, *x*, *pos*) and Fitting of the Data. To assess the fluorophilicity of phosphines **1**, their partition coefficients in the representative solvent system PFMCH/toluene[8] were determined by gravimetric and/or ICP-AAS analysis. Toluene was chosen as the organic phase because it features moderate polarity, dipolar $\pi-\pi$ interactions, and consequently a moderate internal cohesion enthalpy that might be considered representative of the organic phase of a real reaction mixture. It should be kept in mind that an organic solvent of higher polarity will improve the affinity of the fluorous phosphines for the fluorous phase.[1] A 2D representation of the 4D parameter set, containing all experimental partitioning data determined in PFMCH/toluene (1:1, v/v) at 0 °C, is shown in Figure 1.

   For each position, C3, C4, or C3C5, log *P* was fitted separately, resulting in three models that describe most of the observed trends and can be used to predict the missing data (eqs 1−3).

$$\log P_{C4} = -7.6020 + 1.6942a + 3.6379b + 0.3369x - 0.7344ab - 0.1628bx \quad (1)$$

$$\log P_{C3} = -4.4836 + 0.8470a + 0.9315b + 0.1509x \quad (2)$$

$$\log P_{C3C5} = -8.3732 + 2.0411a + 4.1723b + 0.5031x - 0.8435ab - 0.2251bx \quad (3)$$

Under the assumption that the experimental data are normally distributed, qq plots (= plots of log *P* vs the normal distribution) were considered (Figure 2). The resulting straight lines confirm the suitability of this assumption, as well as the validity of the use of a stepwise automatic linear model for the fitting of the data within the class of polynomial models. No higher-order terms of *a*, *b*, and *x* were used, because these terms would have had no direct chemical meaning. The results of the statistical fitting of the data are presented in Tables 2−4. Table 5 lists the predicted log *P* values and compares them with the experimental values. The difference between the predicted and experimentally determined values of log *P* was used as
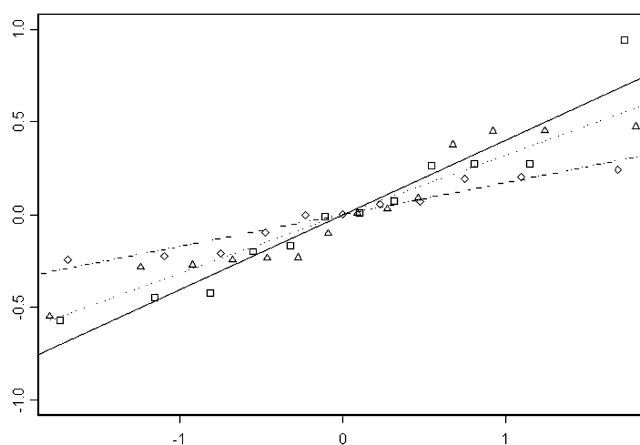
Figure 2. Plot of log *P* vs normal distribution (qq-plot) for *pos* = C3 (□), C4 (△), and C3C5 (◇).

Table 2. Statistical Data[a−c] for Coefficients in Eq 1 for **1**(*a*, *b*, *x*, C4)

term	value	standard error	*t* value	$Pr(>|t|)$
1	−7.6020	2.4580	−3.0927	0.0148
a	1.6942	0.5996	2.8253	0.0223
b	3.6379	1.1360	3.2025	0.0126
x	0.3369	0.1850	1.8204	0.1062
ab	−0.7344	0.2855	−2.5722	0.0330
bx	−0.1628	0.0885	−1.8394	0.1031

   [a] Residual standard error: 0.4205 on eight degrees of freedom. [b] Multiple R^2: 0.7525. [c] *F* statistic: 4.864 on five and eight degrees of freedom; *p* value = 0.024 35.

criterion for the quality of the model. Not surprisingly, in areas of the 4D parameter space where few experimental data points are available, the value of log *P* predicted by the model shows larger uncertainties. This is especially true for phosphines with only one substituted aryl group (*a* = 1). Although two of these phosphines were included in the statistical analysis, based on experimental experience, these type of phosphines were not expected to afford high fluorophilicity and were largely left out of this treatment.

   Trends in the Partition Coefficient and Statistical Models. The previously reported unexpected partitionbehavior of para-substituted phosphines,[6,8] i.e., maxima for *b*

Table 3. Statistical Data^{a-c} for Coefficients in Eq 2 for **1**(a, b, x, C3)

term	value	standard error	t value	$Pr(>|t|)$
1	−4.4836	1.0348	−4.3327	0.0025
a	0.8470	0.2262	3.7450	0.0057
b	0.9315	0.1932	4.8227	0.0013
x	0.1509	0.0966	1.5620	0.1569

^{a} Residual standard error: 0.4849 on eight degrees of freedom.
^{b} Multiple R^2: 0.8425. ^{c} F statistic: 14.27 on three and eight degrees of freedom; p value = 0.001 414.

Table 4. Statistical Data^{a-c} for Coefficients in Eq 3 for **1**(a, b, x, C3C5)

term	value	standard error	t value	$Pr(>|t|)$
1	−8.3732	2.6721	−3.1335	0.0259
a	2.0411	0.9147	2.2314	0.0760
b	4.1723	1.0337	4.0364	0.0100
x	0.5031	0.0872	5.7671	0.0022
ab	−0.8435	0.3414	−2.4706	0.0565
bx	−0.2251	0.0392	−5.7415	0.0022

^{a} Residual standard error: 0.2479 on five degrees of freedom.
^{b} Multiple R^2: 0.9079. ^{c} F statistic: 9.863 on five and five degrees of freedom; p value = 0.012 62.

= 2 rather than $b = 3$ and decreasing log P with increasing x for **1**(3, 3, x, C4), was again observed. This anomalous behavior of the partition coefficient upon variation of the parameters is now supported by an extended number of data points (Figure 1). Equation 1, obtained by fitting of the experimental values of log P to linear functions of the parameters a, b, and x, describes the observed trends. The results of the statistical analysis, showing the goodness of the fit, are given in Table 2. Although b and x are not continuous variables, contour plots of log P vs b and x for $a =$ and 2, 3 are given in Figure 3 as graphical representations of eq 1. A saddle point is observed for the $a = 3$ plot at $b = 2$ and $x = 9$ (log $P = 0.45$).

If all parameters a, b, and x are equal to 0, structure **1**(a, b, x, pos) corresponds to unsubstituted PPh$_3$. The large negative intercept, which equals the value of log P if $a = b = x = 0$, represents the low preference for the fluorous phase of unsubstituted, nonfluorous PPh$_3$ and is present implicitly in the data of Figure 1. The positive effect of an increase in either a, b, or x is counterbalanced by the negative effect of the cross terms ab and bx. Therefore, an increase of a results in an increase of log P if $b = 1$ or 2 and in a decrease of log P if $b = 3$ (Figure 3). An increase of b results in an increase of log P, except in the range $a = 3$, $b \geq 2$, and $x \geq 8$, for which a decrease is observed. Combining the trends observed for a, b, and x results in a high value of log P when only two aryl groups are substituted ($a = 2$) and the silicon atom bears three short fluorinated tails with a maximum at **1**(2, 3, 4, C4).

Any increase of x results in an increase of log P if $b = 1$ and in a decrease if $b = 3$. Increasing tail length, even at $a = 3$, $b = 1$, is predicted to be much less effective than attaching a tris(1H,1H,2H,2H-perfluorohexyl)silyl group in the para positions of two aryl rings ($a = 2$, $b = 3$, $x = 4$), certainly if the number of fluorinated carbons (C_F) is kept the same.

Changing the position of the silicon atom from the para position to the meta position of the aryl ring has a dramatic influence on the value of the partition coefficient, as well as the trends resulting from variations in a, b, and x (Figures 1 and 3). Because cross terms and higher-order terms are absent, the contour plots resulting from eq 2 show straight lines.

The negative intercept again represents a partition coefficient P near 0 for PPh$_3$. The order of importance of the parameters according to the partial derivatives of log P with respect to a, b, and x is $x < a \approx b$. The positive coefficients of a, b, and x in eq 2 indicate that any increase in these parameters results in a higher value of log P (Figures 1 and 3). It should be realized that the standard error is such that the exact position of the maximum [**1**(3, 3, 10, C3), $P = 229$] is not accurately defined. Also **1**(3, 3, 8, C3), **1**(3, 3, 6, C3), and **1**(2, 3, 10, C3) are good candidates.

The use of both meta positions on the aryl rings enabled the synthesis of phosphines containing up to 18 perfluoroalkyl tails. The experimental partition coefficient data measured for **1**(a, b, x, C3C5) (Figure 1 and graphically presented in Figure 3) can be described by eq 3. The statistical data for the coefficients in eq 3, showing the goodness of fit, are given in Table 4. The overall appearance of the contour plots is essentially a repetition of those for C4 except for a general shift to higher partition coefficients, suggesting some relation to the symmetry of the two types of phosphines. Saddle points are observed near (3, 2, 9, C3C5) and (2, 2, 11, C3C5).

Again, the large negative intercept represents a value of P near 0 for the parent triphenylphosphine. The cross term ab shows that increasing the number of tails per aryl ring while also increasing the number of substituted aryl rings results in a negative contribution to log P. Also increasing x at higher b gives a strongly negative effect on log P because of the cross term bx. Although both cross terms are counterbalanced by the single-parameter terms a, b, and x, their effect becomes prominent for $b = 3$. Consequently, in general, $a = 3$ and tail elongation yield higher log P values except when $b = 3$. The highest log P value is expected for **1**(2, 3, 4, C3C5) (log $P = 2.5$) corresponding to substitution of two aryl rings with silyl groups that bear three relatively short 1H,1H,2H,2H-perfluorohexyl tails. Another local maximum can be found at the opposite site of the parameter space: **1**(3, 1, 10, C3C5) (log $P_{exp} = 1.95$, log $P_{pred} = 2.2$) corresponding to a phosphine with all aryl groups substituted by silyl groups that bear only one relatively long 1H,1H,2H, 2H-perfluorododecyl tail. Counterintuitively, the most fluorous compound, **1**(3, 3, 10, C3C5), is, in fact, a local minimum on the log P surface (log $P_{pred} = 1.0$).

Comparison of eqs 1−3 shows that they all have a negative intercept, representing a partition coefficient near 0 for PPh$_3$. The trends observed for pos = C4 and C3C5 show a striking similarity, i.e., the partition coefficient decreases upon elongation of the tails for $b = 3$ and maximum values are found for **1**(2, 3, 4, pos) and **1**(3, 1, 10, pos) with, in general, $P_{C3C5} > P_{C4}$. The similarity can also be observed in a more quantitative sense from a comparison of eqs 1 and 3.

A completely different trend was observed for pos = C3.

Table 5. Predictions of Missing Partitioning Data for **1**(a, b, x, pos) and Comparison of Some Predicted Data with Experimental Values

			pos = C3			pos = C4			pos = C3C5		
a	b	x	log P_{exp}[a]	log P_{pred}[b]	standard error	log P_{exp}[a]	log P_{pred}[c]	standard error	log P_{exp}[a]	log P_{pred}[d]	standard error
1	1	4		−2.10	0.52		−2.31	0.83		−1.89	1.12
1	1	6		−1.80	0.43		−1.96	0.68		−1.34	1.14
1	1	8	−2.00	−1.50	0.41		−1.61	0.58		−0.78	1.17
1	1	10		−1.20	0.48		−1.26	0.55		−0.22	1.21
1	2	4		−1.17	0.46		−0.06	0.47		0.54	0.52
1	2	6		−0.87	0.37		−0.03	0.37		0.64	0.54
1	2	8		−0.57	0.37	−0.11	−0.01	0.31		0.75	0.57
1	2	10		−0.26	0.45		0.01	0.33		0.85	0.61
1	3	4		−0.24	0.48		2.20	0.74		2.97	0.42
1	3	6		0.06	0.41		1.89	0.60		2.62	0.39
1	3	8		0.37	0.42		1.59	0.55		2.28	0.39
1	3	10		0.67	0.51		1.29	0.60		1.93	0.42
2	1	4		−1.25	0.40		−1.35	0.58		−0.69	0.55
2	1	6		−0.95	0.31		−1.00	0.39		−0.14	0.56
2	1	8		−0.65	0.31	−0.92	−0.65	0.27		0.42	0.59
2	1	10		−0.35	0.42	0.08	−0.30	0.30		0.97	0.64
2	2	4		−0.32	0.31		0.17	0.32	0.89	0.89	0.25
2	2	6	0.92	−0.02	0.19		0.19	0.20		1.00	0.26
2	2	8		0.28	0.23		0.21	0.17		1.10	0.29
2	2	10		0.58	0.38		0.24	0.25		1.21	0.34
2	3	4		0.61	0.31		1.69	0.46		2.48	0.24
2	3	6	0.92	0.91	0.23	1.39	1.38	0.29	2.38	2.13	0.18
2	3	8	1.28	1.21	0.29	1.16	1.08	0.29	1.54	1.79	0.18
2	3	10		1.51	0.43		0.78	0.45		1.44	0.24
3	1	4		−0.41	0.40		−0.39	0.47	0.30	0.50	0.20
3	1	6	−0.55	−0.11	0.33	−0.59	−0.04	0.29	1.25	1.06	0.13
3	1	8		0.20	0.36	0.34	0.31	0.22	1.82	1.62	0.13
3	1	10		0.50	0.48	0.43	0.66	0.33	1.95	2.17	0.20
3	2	4	0.80	0.52	0.28	0.90	0.40	0.25		1.25	0.15
3	2	6	1.09	0.83	0.20	0.89	0.42	0.16	1.35	1.35	0.10
3	2	8	1.40	1.13	0.27	0.89	0.44	0.18	1.53	1.46	0.10
3	2	10		1.43	0.43		0.46	0.30		1.56	0.15
3	3	4	1.25	1.46	0.26	0.95	1.18	0.33	1.89	1.99	0.23
3	3	6	1.19	1.76	0.21	0.63	0.88	0.22		1.64	0.17
3	3	8	2.05	2.06	0.30	0.30	0.57	0.33		1.30	0.17
3	3	10		2.36	0.47		0.27	0.53	1.01	0.95	0.23

[a] Experimental log P of **1**(a, b, x, pos) in PFMCH/toluene at 0 °C. [b] log P predicted using eq 2. [c] log P predicted using eq 1. [d] log P predicted using eq 3.

Increases in a, b, or x all result in higher partition coefficients. However, Figure 3 also demonstrates that, when b = 1, the partition coefficients observed for the meta- and para-substituted phosphines are quite similar.

In Figure 4, it can be seen that the silylated aryl rings of the most fluorophilic para- and 3,5-substituted phosphines both have local C_2 symmetry regarding rotation about the P−C_{ipso} bond. This C_2 symmetry is absent for meta-substituted phosphines, which might well be related to the different dependency of their log P values on the parameters a, b, and x compared to their para- and 3,5-substituted analogues. Interestingly, maximum values of P are found for phosphines with high symmetry regarding rotation about the P−C_{ipso} bond (pos = C4, C3C5) combined with low symmetry about the phosphorus atom (a = 1, 2) or, conversely, phosphines with low symmetry regarding rotation about the P−C_{ipso} bond (pos = C3) combined with high symmetry about the phosphorus atom (a = 3).

Although the models described by eqs 1−3 are valid only for partition coefficients of phosphines **1**(a, b, x, pos) in PFMCH/toluene at 0 °C, it is interesting to check their validity for compounds with related structures. There is a strong linear correlation between the partition coefficients of **1**(2, b, 6, C4) and those of the fluorous derivatives of 1,2-bis(diphenylphosphino)ethane (dppe) **5**(2, b, 6, C4),[12] both containing phosphorus atoms with two (1H,1H,2H,2H-perfluoroalkyl)silyl-substituted phenyl groups (Figure 5).

$$\left[CH_2P \left(\left(\hspace{-0.3em} \bigcirc \hspace{-0.3em} \right) - SiMe_{3-b}(CH_2CH_2C_xF_{2x+1})_b \right)_2 \right]_2$$
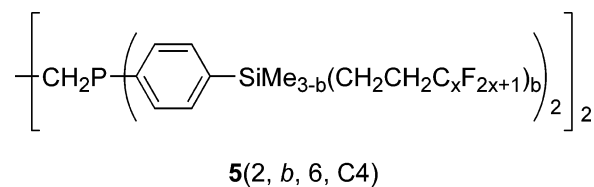
5(2, b, 6, C4)

The experimentally determined partition coefficients of **5**(2, b, 6, C4) can be estimated correctly from the predicted partition coefficients of **1**(2, b, 6, C4) that follow from eq 1 by use of eq 4.

$$\log P_{5(2, b, 6, C4)} = 0.911(\log P_{1(2, b, 6, C4)}) + 0.586 \quad (4)$$
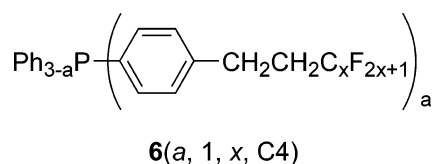
Figure 5 and eq 4 show that the trend observed for increasing b, predicted by eq 1 for monophosphines **1**(a, b, x, pos), is also followed for diphosphines **5**(2, b, 6, C4). If
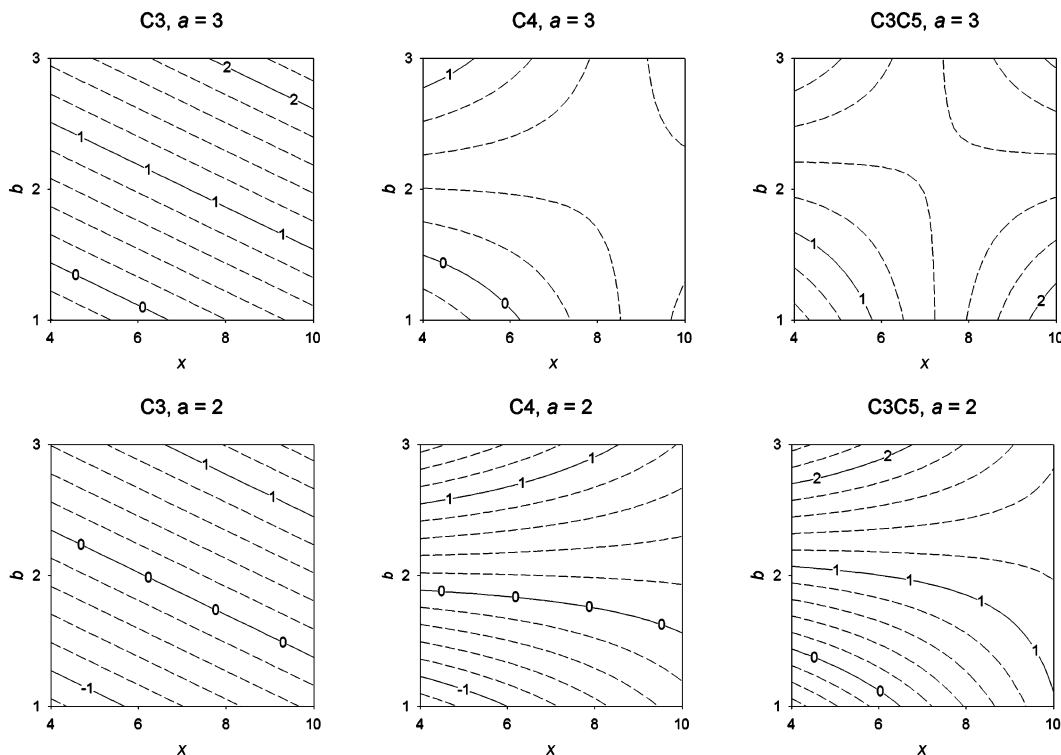
Figure 3. Contour plots of log P $\mathbf{1}(a, b, x, pos)$ vs b and x for $a = 2$ and 3 derived from eqs 1−3.

such relationships could be proven to be more general, then the models from eqs 1−3 could be used for the optimization of alkylarylphosphines, fluorous derivatives of dppe, and possibly α,ω-bis(diphenylphosphino)alkanes as well. On the basis of these assumptions, an optimal partition coefficient is expected for fluorous bis(diaryl)phosphines containing $-Si(CH_2CH_2C_4F_9)_3$ substituents on all meta positions of the aryl rings.

Similarly, reported partition coefficients of $\mathbf{6}(a, 1, 6, C4)$ were compared with those predicted for $\mathbf{1}(a, 1, 6, C4)$ (Figure 6).

$$\text{Ph}_{3-a}\text{P}\left(\!\!\left(\!\!\!\left\langle\!\!\!\bigcirc\!\!\!\right\rangle\!\!\!-\text{CH}_2\text{CH}_2\text{C}_x\text{F}_{2x+1}\right)\!\!\right)_a$$

$\mathbf{6}(a, 1, x, C4)$

Although the values used for comparison were measured at a different temperature and in a different biphasic solvent system using a non-silyl-substituted phosphine, the linear relationship in this case is also remarkable (eq 5).

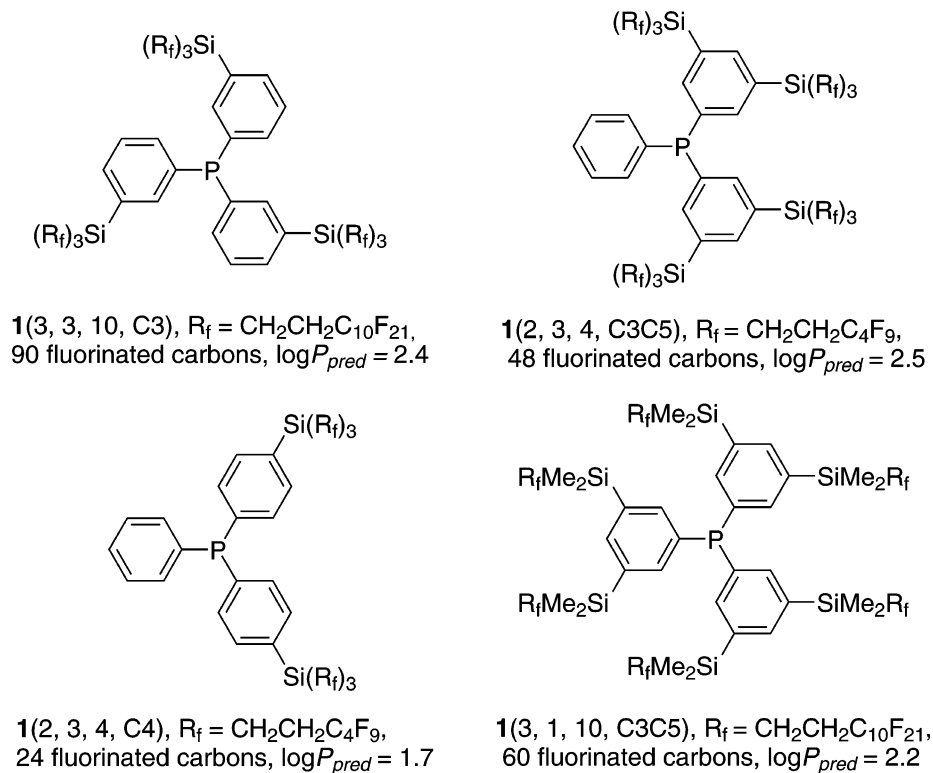$$\log P_{\mathbf{6}(a, 1, 6, C4)} = 1.250(\log P_{\mathbf{1}(a, 1, 6, C4)}) + 1.528 \quad (5)$$

Again, if eq 5 proves to be of more general validity, the partition coefficient can be further optimized by elongation of the tail. For example, a partition coefficient of $P = 82$ can be expected for $\mathbf{6}(3, 1, 8, C4)$, compared to $P = 30$ reported for $\mathbf{6}(3, 1, 6, C4)$. Furthermore, meta- or 3,5-substitution most likely will result in a further increase of the partition coefficient, analogous to the observations for $\mathbf{1}(3, 1, x, pos)$.

Application in Catalysis. The effect of the improved partition coefficients on catalyst leaching was studied in

fluorous biphasic hydrosilylation. For practical purposes, a good balance between solubility and partitioning is required, i.e., the ligand with the highest partition coefficient does not always give the best results in the actual catalytic application because of its possible low solubility. Therefore, one of the better phosphines, i.e., $\mathbf{1}(3, 1, 8, C3C5)$ ($P = 65$), was applied in the fluorous hydrosilylation of 1-hexene (Scheme 4) in PFMCH using the substrates as the organic phase. Reactions were performed under homogeneous conditions, as described previously for less fluorophilic phosphines.[9] In contrast to the previously reported synthesis of fluorous derivatives of Wilkinson's catalyst containing $\mathbf{1}(3, 1, 6, C4)$ or $\mathbf{1}(3, 2, 8, C4)$ as the ligand,[9] $\mathbf{1}(3, 1, 8, C3C5)$ did not react completely with $[RhCl(COD)]_2$.[13] The catalyst was thus synthesized by adding a solution of $\mathbf{1}(3, 1, 8, C3C5)$ in PFMCH to a solution of $[RhCl(COE)_2]_2$ (COE = cyclooctene) in CH_2Cl_2. After the mixture had been stirred, a colorless organic layer was obtained. Removal of the organic layer and evaporation of the fluorous layer to dryness yielded a red oil.

Full conversion of $HSiMe_2Ph$ was obtained after 15 min (Table 6), showing that the rhodium catalyst containing $\mathbf{1}(3, 1, 8, C3C5)$ is as active as the previously reported catalysts containing $\mathbf{1}(3, 1, 6, C4)$, $\mathbf{1}(3, 2, 8, C4)$, or PPh_3. The starting alkene was completely converted to the anti-Markovnikov product, and some of the excess of 1-hexene was isomerized toward 2-hexenes (15%).

Three cycles were performed, and no drop in activity or selectivity was observed upon recycling. Leaching of rhodium and phosphorus was investigated by ICP-AAS. As becomes clear from the data in Table 6, a higher partition coefficient of the free fluorous phosphine indeed leads to a lower amount of leaching of the fluorous catalyst, despite the different biphasic solvent system and separation temperature employed during the measurements of the partition

1(3, 3, 10, C3), $R_f = CH_2CH_2C_{10}F_{21}$,
90 fluorinated carbons, $\log P_{pred} = 2.4$

1(2, 3, 4, C3C5), $R_f = CH_2CH_2C_4F_9$,
48 fluorinated carbons, $\log P_{pred} = 2.5$

1(2, 3, 4, C4), $R_f = CH_2CH_2C_4F_9$,
24 fluorinated carbons, $\log P_{pred} = 1.7$

1(3, 1, 10, C3C5), $R_f = CH_2CH_2C_{10}F_{21}$,
60 fluorinated carbons, $\log P_{pred} = 2.2$

Figure 4. Structures of **1**(3, 1, *x*, *pos*) showing different symmetries for *pos* = C4/C3C5 and C3.
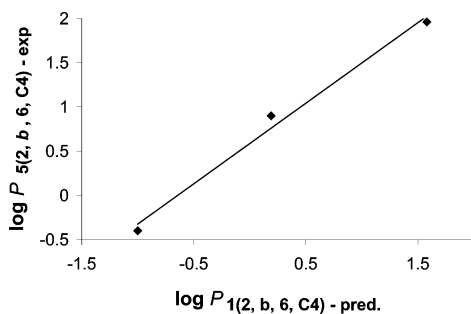
Figure 5. Prediction of $\log P_{5(2, b, 6, C4)}$[12] from $\log P_{1(2, b, 6, C4)-pred}$ in PFMCH/toluene at 0 °C.
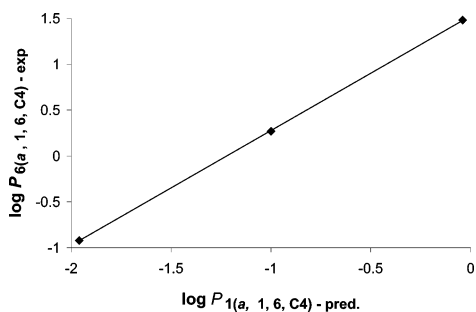
Figure 6. Prediction of $\log P_{6(a, 1, 6, C4)}$[4g] in FC-72/MeOH at room temperature from $\log P_{1(a, 1, 6, C4)-pred}$ in PFMCH/toluene at 0 °C.

coefficients of the free ligands. Whereas 12% rhodium leaching was found for **1**(3, 1, 6, C4), no rhodium was detected in the organic layer by ICP-AAS using **1**(3, 1, 8, C3C5) as the ligand. Also, the amount of leaching of the free fluorous ligand was decreased by an order of magnitude. Interestingly, comparison with leaching data obtained earlier for **1**(3, 2, 8, C4), which contains an equal number of perfluoroalkyl tails of the same length as **1**(3, 1, 8, C3C5),

shows that the position of the silicon atom on the aryl ring and the specific arrangement of the tails around the phosphorus donor atom have a marked effect on catalyst leaching.
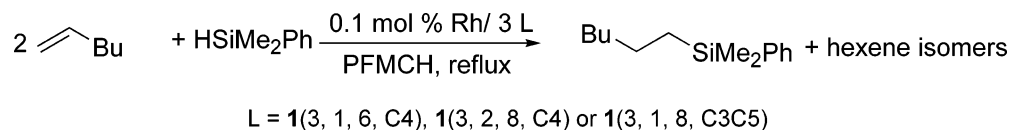
Conclusions

By varying the number of substituted phenyl groups (*a*), the number of fluorous tails per silicon (*b*), the length of the tails (*x*), and the position of the silicon atom on the aryl ring (*pos*), a library of silyl-substituted fluorous derivatives of triphenylphosphine was prepared using combinatorial techniques. The partition coefficients of individual library members in a typical fluorous biphasic system were determined. Meta-substituted fluorous phosphines exhibited regular behavior, i.e., in most cases, longer and more tails led to higher preference for the fluorous phase. Para- and 3,5-substituted phosphines showed irregular behavior in the sense that elongation of tails or an increase in the number of tails did not necessarily lead to higher partition coefficients. High experimental values of the partition coefficient were found for **1**(3, 3, 4, C3C5), **1**(3, 1, 10, C3C5), **1**(2, 3, 6, C3C5), and **1**(3, 3, 8, C3). Except for **1**(3, 1, 10, C3C5), these compounds all contain 72 fluorinated carbon atoms at the meta position(s) of the aryl rings. Even higher values of log *P* are statistically predicted for **1**(2, 3, 4, C3C5) and **1**(3, 3, 10, C3).

Using a combination of statistical analysis and combinatorial methods, the substitution pattern resulting in high partition coefficients was optimized quickly without preparation of all possible compounds. The partition coefficient was increased by more than an order of magnitude, from an initial maximum of $P = 7.8$ for **1**(3, 2, 6, C4)[8] to an optimized and experimentally confirmed value of $P > 238$ for **1**(2, 3, 6, C3C5).

Scheme 4

$$2 \nearrow \text{Bu} \quad + \text{HSiMe}_2\text{Ph} \xrightarrow[\text{PFMCH, reflux}]{0.1 \text{ mol \% Rh/ 3 L}} \text{Bu} \diagdown\diagup \text{SiMe}_2\text{Ph} \quad + \text{hexene isomers}$$

L = **1**(3, 1, 6, C4), **1**(3, 2, 8, C4) or **1**(3, 1, 8, C3C5)

Table 6. Application of Three Library Members **1**(*a, b, x, pos*) in Fluorous Rhodium−Catalyzed Hydrosilylation[a]

ligand	P^b	conversion (%) (reaction time)	no. of cycles	leaching[c]	
				Rh	P
1(3, 1, 6, C4)[d]	0.26	100 (15 min)	3	12%, 41 ppm	19%, 58 ppm
1(3, 2, 8, C4)[d]	7.8	100 (15 min)	3	1.7%, 5.7 ppm	2.2%, 6.6 ppm
1(3, 1, 8, C3C5)	65	100 (15 min)	3	<0.1%, <1 ppm	0.8%, 7 ppm

[a] Conditions: catalyst/silane/1-hexene = 1:1000:2000, reflux, PFMCH solvent, [Rh] = 2 mM. [b] For conditions, see Figure 1. [c] Phase separation at room temperature, determined by ICP-AAS. [d] Data from ref 9.

The linear relationship between log P of **1**(*a, b, x*, C4) and **5**(2, *b*, 6, C4) or **6**(*a*, 1, 6, C4) suggests that the observed trends for **1**(*a, b, x, pos*) described by eqs 1−3 can also be used for optimization of other fluorous phosphine ligands.

Compound **1**(3, 1, 8, C3C5) was successfully applied in the fluorous, rhodium-catalyzed hydrosilylation of 1-hexene. No differences in activity and selectivity were observed compared to the previously reported fluorous catalysts or [RhCl(PPh$_3$)$_3$]. More importantly, optimization of the partition coefficient of the fluorous ligand in PFMCH/toluene resulted in a significant decrease of catalyst leaching, as well as leaching of free fluorous ligand.

From the data presented above, it might be obvious that not only the total number of tails and the length (*x*) of each tail are important, but also the specific substitution pattern/ shape of the molecule. For this reason, relationships predicting the partition coefficient P solely from the (specific) molar volume and the Hildebrand solubility or nonspecific internal cohesion parameter[6,7] should be considered as a first approximation for estimation of log P, given that they do not account for the observed differences in the partition coefficients of isomers.

Experimental Section

General. All experiments were performed in a dry dinitrogen atmosphere using standard Schlenk techniques. Solvents were stored over sodium benzophenone ketyl and distilled before use. Fluorinated solvents [*c*-CF$_3$C$_6$F$_{11}$ (Lancaster) and FC-72 (Acros)] were degassed and stored under dinitrogen atmosphere. Compounds C$_x$F$_{2x+1}$CH$_2$CH$_2$SiMe$_2$-Cl (*x* = 4, 6, 8, or 10),[9] (C$_x$F$_{2x+1}$CH$_2$CH$_2$)$_b$SiMe$_{3-b}$Br (*b* = 2, 3; *x* = 6, 8),[8] (C$_{10}$F$_{21}$CH$_2$CH$_2$)$_3$SiBr,[10] Ph$_{3-a}$P(C$_6$H$_4$Br-*4*)$_a$ (*a* = 1−3),[8] Ph$_2$P(C$_6$H$_4$Br-*3*),[11] and **1**(3, *b, x*, C4) (*b* = 1−3; *x* = 6, 8)[8] were prepared as reported. Other chemicals were obtained from commercial suppliers (Acros, Aldrich, Lancaster) and used as delivered. Microanalyses were carried out by H. Kolbe, Mikroanalytisches Laboratorium, Mülheim an der Ruhr, Germany. ^{31}P NMR spectra were externally referenced against H$_3$PO$_4$ (δ = 0 ppm). Parallel syntheses were performed using a Quest 210 semiautomatic parallel synthesizer (Argonaut Technologies), connected to a Julabo F83-MV cryostat via two 3-m isolated tubes.

General Experimental Procedure for the Synthesis of (C$_x$F$_{2x+1}$CH$_2$CH$_2$)$_b$SiMe$_{3-b}$H [2(*b, x*) (*b* = 2, 3)]. To a suspension of Mg turnings (15−20 g) in Et$_2$O (250 mL) was

added a solution of C$_x$F$_{2x+1}$CH$_2$CH$_2$I (25 g; *x* = 4, 6, 8, 10) in Et$_2$O (100 mL), and the mixture was stirred vigorously overnight. Subsequently, the Grignard solution was removed by syringe, and HSiMe$_{3-b}$Cl$_b$ (*b* = 2, 3) was added. After the mixture had been stirred overnight, the reaction was quenched with aqueous HCl. The phases were separated, the aqueous layer was washed with Et$_2$O, and the collected organic layers were dried over MgSO$_4$. Filtration, evaporation of the solvent, and (Kugelrohr) distillation of the remaining oil (*x* = 4, 6) or washing of the remaining solid with pentane (*x* = 8, 10) yielded **2**(*b, x*) containing some Wurtz coupling product (0−25%).

2(2, 4). C$_4$F$_9$CH$_2$CH$_2$I (25 g, 67 mmol), Mg (17.3 g, 0.712 mol), and HSiMeCl$_2$ (2.69 g, 23.4 mmol) yielded 2.10 g (17% relative to HSiMeCl$_2$) of a colorless liquid, containing 25% of (C$_4$F$_9$CH$_2$CH$_2$)$_2$ after two vacuum distillations. bp (0.1 mbar) 97 °C. ^{1}H NMR [200 MHz, C$_6$D$_6$/C$_6$F$_6$ (1:1)]: δ −0.06 (d, 3H, $^3J_{HH}$ = 2.80 Hz), 0.68 (m, 4H), 1.91 (m, 4H), 3.74 (m, 1H).

2(3, 4). C$_4$F$_9$CH$_2$CH$_2$I (25 g, 67 mmol), Mg (18 g, 0.741 mol), and HSiCl$_3$ (2.10 g, 15.5 mmol) yielded 7.86 g (66% relative to HSiCl$_3$) of a colorless liquid, containing 8% of (C$_4$F$_9$CH$_2$CH$_2$)$_2$ after vacuum distillation. bp (0.1 mbar) 159 °C. ^{1}H NMR (200 MHz, CDCl$_3$): δ 0.97 (m, 6H), 2.12 (m, 6H), 3.94 (m, 1H).

2(2, 10). C$_{10}$F$_{21}$CH$_2$CH$_2$I (25 g, 37 mmol), Mg (17.5 g, 0.720 mol), and HSiMeCl$_2$ (1.21 g, 10.5 mmol) yielded 4.90 g (41% relative to HSiMeCl$_2$) of a white solid, which was further purified by Kugelrohr distillation (0.1 mbar, 140 °C). ^{1}H NMR [200 MHz, C$_6$D$_6$/C$_6$F$_6$ (1:1)]: δ −0.04 (d, 3H, $^3J_{HH}$ = 2.70 Hz), 0.70 (m, 4H), 1.92 (m, 4H), 3.77 (m, 1H).

General Experimental Procedure for the Synthesis of (C$_x$F$_{2x+1}$CH$_2$CH$_2$)$_b$SiMe$_{3-b}$Br [3(*b, x*) (*b* = 2, 3)]. To a solution of **2**(*b, x*) in hexanes (*x* = 4, 6, 8) or hexanes/FC-72 (3:1, *x* = 10) was added Br$_2$. The mixture was stirred for 15 h, and all volatiles were evaporated. The residue was dissolved in a toluene/FC-72 [1:3 (v/v)] biphasic system. Phase separation and evaporation of the fluorous phase afforded the fluorous bromosilanes **3**(*b, x*) as a colorless oil (*x* = 4, 6) or a white solid (*x* = 8, 10).

3(2, 4). **2**(2, 4) (2.10 g, 3.90 mmol) and Br$_2$ (3.0 g, 19 mmol) yielded 2.40 g (99%) of a colorless liquid containing 25% of (C$_4$F$_9$CH$_2$CH$_2$)$_2$. ^{1}H NMR (200 MHz, CDCl$_3$): δ 0.19 (s, 3H), 1.09 (m, 6H), 2.10 (m, 6H).

3(3, 4). **2**(3, 4) (7.86 g, 10.2 mmol) and Br$_2$ (3.0 g, 19

mmol) yielded 8.49 g (98%) of a colorless liquid containing 8% of $(C_4F_9CH_2CH_2)_2$. ^{1}H NMR (200 MHz, CDCl$_3$): δ 1.27 (m, 6H), 2.19 (m, 6H).

3(2, 10). **2**(2, 10) (4.90 g, 4.31 mmol) and Br$_2$ (3.0 g, 19 mmol) yielded 5.02 g (96%) of a white solid.^{1}H NMR [200 MHz, C$_6$D$_6$/C$_6$F$_6$ 1:1 (v/v)]: δ 0.12 (s, 3H), 0.88 (m, 6H), 1.97 (m, 6H).

General Experimental Procedure for the Synthesis of Bromo-Substituted Derivatives of PPh$_3$ [4(*a*, *pos*) (*a* = 2, 3; *pos* = C3, C3C5)]. To a solution of *m*-C$_6$H$_4$Br$_2$ in THF or a suspension of 1,3,5-C$_6$H$_3$Br$_3$ in Et$_2$O at −90 °C was added 1 equiv of *n*-BuLi. After the mixture had been stirred for 30 min, 1/*a* equiv of Ph$_{3-a}$PCl$_a$ was added over 2 h while the temperature was kept below −80 °C. After this mixture had been stirred at 25 °C for 15 h, all volatiles were evaporated, and the residue was dissolved in water/CH$_2$Cl$_2$. Phase separation, drying of the organic layer over MgSO$_4$, filtration, and evaporation to dryness yielded white or light yellow solids, which were further purified by precipitation from hexanes.

4(2, C3). *m*-C$_6$H$_4$Br$_2$ (12.03 g, 51.0 mmol), 33.1 mL of a pentane solution of *n*-BuLi (1.54 M, 51.0 mmol), and PPhCl$_2$ (4.56 g, 25.5 mmol) yielded 7.03 g (33%) of a white/yellow sticky solid. ^{1}H NMR (200 MHz, CDCl$_3$): δ 7.26 (m, 4H), 7.37−7.53 (m, 9H). ^{31}P NMR (81 MHz, CDCl$_3$): δ −3.5. Anal. Calcd. for C$_{18}$H$_{13}$Br$_2$P: C 51.46, H 3.12, P 7.37. Found: C 51.45, H 3.20, P 7.31.

4(3, C3). *m*-C$_6$H$_4$Br$_2$ (9.10 g, 38.6 mmol), 24.9 mL of a pentane solution of *n*-BuLi (1.54 M, 38.6 mmol), and PCl$_3$ (1.77 g, 12.9 mmol) yielded 3.98 g (62%) of a white solid. mp 117−119 °C. ^{1}H NMR (200 MHz, CDCl$_3$): δ 7.22 (m, 6H), 7.41 (d, 3H, $^3J_{HP}$ = 7.2 Hz), 7.51 (m, 3H). ^{13}C NMR (50.3 MHz, CDCl$_3$): δ 123.5 (d, $^3J_{PC}$ = 7.9 Hz), 130.5 (d, $^3J_{PC}$ = 6.9 Hz), 132.2 (d, $^2J_{PC}$ = 19.3 Hz), 132.6 (s), 136.2 (d, $^2J_{PC}$ = 22.1 Hz), 138.6 (d, $^1J_{PC}$ = 15.2 Hz). ^{31}P NMR (81 MHz, CDCl$_3$): δ −3.2. Anal. Calcd. for C$_{18}$H$_{12}$Br$_3$P: C 43.33, H 2.42, P 6.21. Found: C 43.22, H 2.45, P 6.26.

4(2, C3C5). 1,3,5-C$_6$H$_3$Br$_3$ (4.56 g, 14.5 mmol), 9.1 mL of a pentane solution of *n*-BuLi (1.6 M, 14.5 mmol), and PPhCl$_2$ (1.30 g, 7.24 mmol) yielded 3.81 g (91%) of a white/yellow solid. mp 92−95 °C. ^{1}H NMR (200 MHz, CDCl$_3$): δ 7.35 (dd, 4H, $^4J_{HH}$ = 1.60 Hz; $^3J_{HP}$ = 7.00 Hz), 7.41 (m, 5H), 7.67 (t, 2H, $^4J_{HH}$ = 1.60 Hz). ^{31}P NMR (81 MHz, CDCl$_3$): δ −2.0. Anal. Calcd. for C$_{18}$H$_{11}$Br$_4$P: C 37.41, H 1.92, P 5.36. Found: C 37.49, H 1.94, P 5.33.

4(3, C3C5). 1,3,5-C$_6$H$_3$Br$_3$ (6.46 g, 20.5 mmol), 12.8 mL of a pentane solution of *n*-BuLi (1.54 M, 20.5 mmol), and PCl$_3$ (0.94 g, 6.84 mmol) yielded 4.78 g (95%) of a white solid. mp 128−130 °C. ^{1}H NMR (200 MHz, CDCl$_3$): δ 7.30 (dd, 6H, $^4J_{HH}$ = 1.80 Hz; $^3J_{HP}$ = 7.20 Hz), 7.72 (t, $^4J_{HH}$ = 1.80 Hz). ^{31}P NMR (81 MHz, CDCl$_3$): δ −1.4. Anal. Calcd. for C$_{18}$H$_9$Br$_6$P: C 29.39, H 1.23, P 4.21. Found: C 29.36, H 1.28, P 4.26.

Statistical Procedures: Selection prior to Synthesis and Analysis of the Dataset Afterward. The first block consisted of the six published compounds **1**(3, *b*, *x*, C4)[8] with three additional meta-substituted phosphines **1**(3, *b*, 6, C3). Initially, it was thought that a standard orthogonal fraction obtained by a $2^2 \times 3^3$ design should be performed,[14] with

most of the points of the first block embedded. The second block was selected from such a fraction. Because the thus-obtained data indicated that optimized values were not expected for some regions (e.g., *a* = 1), these regions were not considered further in the subsequent blocks. Therefore, and because of the nonuniformity of the two blocks so far, it was decided that orthogonality of the design would no longer be pursued, and the data were then analyzed per position. A crude version of the steepest ascent method, based on the data for the first and second blocks, was used for the selection of the phosphines for the third and subsequently the fourth block, resulting in a total library of 37 members.

The statistical package Splus was used for both the analysis and the selection of the orthogonal fraction. The data points obtained for a constant value of *pos* were fitted using stepwise regression analysis. In this way, a best fit was obtained for each value of *pos*. Statistical criteria for a good fit were the residuals; the standard errors of the coefficients and their $Pr(> |t|)$ values; and the R^2, F, and p values of the fit. A linear fit was preferred over a nonlinear fit, given that nonlinear terms have no direct chemical meaning. Furthermore, a good fit was likely to have a negative intercept. The predictions of known data points should be close to the experimental data with standard errors as small as possible and they should describe the observed trends.

General Experimental Procedure for the Parallel Synthesis of 1(*a*, *b*, *x*, C4) and 1(*a*, *b*, *x*, C3). Ten 10-mL reaction vials with filters were flushed with nitrogen gas for 1 h and subsequently charged with **4**(*a*, *pos*), which was dissolved in Et$_2$O. The solutions were cooled to −40 °C and continuously agitated every 0.7 s. The maximum height of the magnetic bars was adjusted to the height of the solution. Subsequently, 2.3*a* equiv of *t*-BuLi (0.75 M solution in pentane) was added, and the formed suspension was agitated for 1 h. A solution of fluorous silyl halide **3**(*b*, *x*) (*a* equiv) in Et$_2$O was added. After 30 min, the temperature was raised to 25 °C, and the agitation frequency was lowered to 1 Hz. Degassed water was added after 15 h. The water layer was removed by opening the taps in the lower manifold, and MgSO$_4$ was added to all vials. The organic layers were collected in 10 separate, weighed Schlenk vessels by opening the lower manifold tap, allowing filtration. The MgSO$_4$ was washed twice with Et$_2$O, and the collected organic layers were evaporated to dryness. For yields and ^{1}H and ^{31}P NMR data, see Table 7.

1(1, 1, 8, C3): Anal. Calcd. for C$_{30}$H$_{24}$F$_{17}$PSi: C 47.01, H 3.16, P 4.04, F 42.13. Found: C 47.34, H 3.22, P 4.18, F 42.04.

1(3, 1, 6, C3): Anal. Calcd. for C$_{48}$H$_{42}$F$_{39}$PSi$_3$: C 39.08, H 2.87, F 50.24, P 2.10. Found: C 39.19, H 2.96, F 50.39, P 2.17. ^{13}C NMR (50.3 MHz, CDCl$_3$): δ −3.5 (s), 5.3 (s), 25.9 (t, $^2J_{CF}$ = 23.3 Hz), 103.8−126.7 (m), 128.3 (d, $^3J_{PC}$ = 6.0 Hz), 134.0 (s), 134.6 (d, $^2J_{PC}$ = 16.6 Hz), 136.7 (d, $^1J_{PC}$ = 11.5 Hz), 137.8 (d, $^3J_{PC}$ = 6.0 Hz), 138.9 (d, $^2J_{PC}$ = 22.1 Hz). ^{19}F NMR [282 MHz, C$_6$D$_6$/C$_6$F$_6$ (1:1)]: δ −82.3 (m, 9F), −117.3 (m, 6F), −123.3 (m, 12F), −124.3 (m, 6F), −127.7 (m, 6F).

1(3, 2, 6, C3): Anal. Calcd. for C$_{69}$H$_{45}$F$_{78}$PSi$_3$: C 33.54, H 1.84, F 59.97, P 1.25. Found: C 33.52, H 1.77, F 60.11,

Table 7. Analytical Data for the Newly Prepared Fluorous Triarylphosphines **1**

compound	yield (%)	^{31}P NMR δ	^{1}H NMR (C_6D_6/C_6F_6, 1:1) δ
1(1, 1, 8, C3)	84	−4.0	0.23 (s, 6H), 0.86 (m, 2H), 1.93 (m, 2H), 7.16 (m, 12H), 7.34 (d, 1H, $^{3}J_{HP}$ = 6.8 Hz), 7.48 (d, 1H, $^{3}J_{HP}$ = 7.8 Hz)
1(2, 2, 6, C3)	90	−4.6	0.17 (s, 6H), 0.90 (m, 8H), 1.93 (m, 8H), 7.25 (m, 13H)
1(2, 3, 4, C3)	76	−4.6	0.94 (m, 12H), 1.95 (m, 12H), 7.21 (m, 11H), 7.39 (d, 2H, $^{3}J_{HP}$ = 7.2 Hz)
1(2, 3, 6, C3)	81	−4.6	0.96 (m, 12H), 1.96 (m, 12H), 7.2−7.4 (m, 13H)
1(2, 3, 8, C3)	81	−4.6	1.00 (m, 12H), 2.00 (m, 12H), 7.15−7.40 (m, 13H)
1(2, 3, 10, C3)	94	−3.8	0.92 (m, 12H), 2.10 (m, 12H), 7.2−7.6 (m, 13H)
1(3, 1, 6, C3)	94	−4.7	0.24 (s, 18H), 0.90 (m, 6H), 2.02 (m, 6H), 7.37 (m, 12H)
1(3, 2, 4, C3)	92	−4.7	0.14 (s, 9H), 0.91 (m, 12H), 1.95 (m, 12H), 7.20−7.35 (m, 9H), 7.49 (d, 3H, $^{3}J_{HP}$ = 7.8 Hz)
1(3, 2, 6, C3)	67	−4.8	0.25 (s, 9H), 0.93 (m, 12H), 1.92 (m, 12H), 7.31 (m, 12H)
1(3, 2, 8, C3)	86	−4.8	0.21 (s, 9H), 1.00 (m, 12H), 1.95 (m, 12H), 7.34 (m, 12H)
1(3, 3, 4, C3)	82	−4.5	0.99 (m, 18H), 1.95 (m, 18H), 7.32 (m, 9H), 7.58 (d, 3H, $^{3}J_{HP}$ = 7.8 Hz)
1(3, 3, 6, C3)	63	−4.7	1.00 (m, 18H), 2.02 (m, 18H), 7.47 (m, 12H)
1(3, 3, 8, C3)	86	−4.6	0.99 (m, 18H), 2.02 (m, 18H), 7.36 (m, 9H), 7.54 (d, 3H, $^{3}J_{HP}$ = 7.6 Hz)
1(1, 2, 8, C4)	95	−3.9	0.23 (s, 3H), 1.00 (m, 4H), 2.03 (m, 4H), 7.1−7.3 (m, 14H)
1(2, 1, 8, C4)	72	−4.1	0.23 (s, 12H), 0.93 (m, 4H), 2.00 (m, 4H), 7.14−7.30 (m, 13H)
1(2, 1, 10, C4)	87	−4.1	0.23 (s, 12H), 0.91 (m, 4H), 2.00 (m, 4H), 7.15−7.31 (m, 13H)
1(2, 2, 6, C4)	72	−4.5	0.21 (s, 6H), 0.95 (m, 8H), 1.97 (m, 8H), 7.0−7.5 (m, 13H)
1(2, 3, 6, C4)	78	−4.0	1.01 (m, 12H), 2.03 (m, 12H), 7.24 (m, 13H)
1(2, 3, 8, C4)	75	−4.0	1.08 (m, 12H), 2.04 (m, 12H), 7.25 (m, 13H)
1(3, 1, 10, C4)	40	−4.3	0.23 (s, 18H), 0.98 (m, 6H), 2.02 (m, 6H), 7.30 (m, 12H)
1(3, 2, 4, C4)	98	−4.4	0.23 (s, 9H), 0.97 (m, 12H), 1.97 (m, 12H), 7.24 (m, 12H)
1(3, 3, 4, C4)	87	−4.3	0.99 (m, 18H), 2.02 (m, 18H), 7.29 (m, 12H)
1(3, 3, 10, C4)	86	−3.9	0.91 (m, 18H), 1.90 (m, 18H), 7.18 (m, 12H)
1(2, 2, 4, C3C5)	85	−4.8	0.16 (s, 12H), 0.93 (m, 18H), 1.91 (m, 18H), 7.23 (m, 5H), 7.54 (d, 4H, $^{3}J_{HP}$ = 7.4 Hz), 7.65 (s, 2H)
1(2, 2, 10, C3C5)	75	−4.6	0.15 (s, 12H), 0.90 (m, 18H), 1.95 (m, 18H), 7.26 (m, 5H), 7.51 (d, 4H, $^{3}J_{HP}$ = 7.3 Hz), 7.62 (s, 2H)
1(2, 3, 6, C3C5)	80	−4.7	1.03 (m, 24H), 2.00 (m, 24H), 7.30 (m, 5H), 7.61 (d, 4H, $^{3}J_{HP}$ = 7.0 Hz), 7.68 (s, 2H)
1(2, 3, 8, C3C5)	94	−4.7	1.10 (m, 24H), 2.02 (m, 24H), 7.32 (m, 5H), 7.63 (d, 4H, $^{3}J_{HP}$ = 7.0 Hz), 7.73 (s, 2H)
1(3, 1, 4, C3C5)	89	−5.1	0.22 (s, 36H), 0.94 (m, 12H), 2.02 (m, 12H), 7.54 (d, 6H, $^{3}J_{HP}$ = 7.0 Hz), 7.75 (s, 3H)
1(3, 1, 6, C3C5)	69	−5.0	0.21 (s, 36H), 0.89 (m, 12H), 1.99 (m, 12H), 7.51 (d, 6H, $^{3}J_{HP}$ = 7.2 Hz), 7.72 (s, 3H)
1(3, 1, 8, C3C5)	97	−5.2	0.21 (s, 36H), 0.93 (m, 12H), 2.03 (m, 12H), 7.56 (d, 6H, $^{3}J_{HP}$ = 7.0 Hz), 7.76 (s, 3H)
1(3, 1, 10, C3C5)	94	−5.3	0.19 (s, 36H), 0.91 (m, 12H), 2.01 (m, 12H), 7.56 (d, 6H, $^{3}J_{HP}$ = 7.0 Hz), 7.74 (s, 3H)
1(3, 2, 6, C3C5)	88	−4.2	0.21 (s, 18H), 1.06 (m, 24H), 2.02 (m, 24H), 7.61 (d, 6H, $^{3}J_{HP}$ = 7.0 Hz), 7.75 (s, 3H)
1(3, 2, 8, C3C5)	82	−4.1	0.19 (s, 18H), 1.05 (m, 24H), 2.02 (m, 24H), 7.58 (d, 6H, $^{3}J_{HP}$ = 6.9 Hz), 7.73 (s, 3H)
1(3, 3, 4, C3C5)	78	−1.1	1.08 (m, 36H), 2.09 (m, 36H), 7.69 (d, 6H, $^{3}J_{HP}$ = 7.0 Hz), 7.79 (s, 3H)
1(3, 3, 10, C3C5)	71	−3.7	1.02 (m, 36H), 2.09 (m, 36H), 7.2−7.6 (m, 9H)

P 1.32. ^{13}C NMR (50.3 MHz, CDCl$_3$): δ −6.5 (s), 3.5 (s), 25.8 (t, $^{2}J_{CF}$ = 23.8 Hz), 107.8−123.7 (m), 128.9 (d, $^{3}J_{PC}$ = 5.4 Hz), 134.4 (s), 135.2 (d, $^{3}J_{PC}$ = 5.5 Hz), 135.2 (d, $^{2}J_{PC}$ = 16.5 Hz), 137.3 (d, $^{1}J_{PC}$ = 12.8 Hz), 139.0 (d, $^{2}J_{PC}$ = 22.0 Hz). ^{19}F NMR [282 MHz, C$_6$D$_6$/C$_6$F$_6$ (1:1)]: δ −83.0 (m, 18F), −117.5 (m, 12F), −123.3 (m, 24F), −124.4 (m, 12F), −127.8 (m, 12F).

1(3, 3, 4, C3): Anal. Calcd. for C$_{72}$H$_{48}$F$_{81}$PSi$_3$: C 33.68, H 1.88, F 59.94, P 1.21. Found: C 33.82, H 1.96, F 59.86, P 1.16.

1(3, 3, 6, C3): Anal. Calcd. for C$_{90}$H$_{48}$F$_{117}$PSi$_3$: C 31.17, H 1.40, F 64.11, P 0.89. Found: C 31.26, H 1.45, F 64.03, P 0.96. ^{13}C NMR [50.3 MHz, C$_6$D$_6$/C$_6$F$_6$ (1:1)]: δ 1.8 (s), 26.1 (t, $^{2}J_{CF}$ = 23.8 Hz), 106.1−120.2 (m), 129.7 (s), 133.7 (d, $^{3}J_{PC}$ = 6.1 Hz), 135.2 (s), 135.9 (d, $^{2}J_{PC}$ = 14.0 Hz), 138.7 (d, $^{1}J_{PC}$ = 14.6 Hz), 139.9 (d, $^{2}J_{PC}$ = 23.8 Hz). ^{19}F NMR [282 MHz, C$_6$D$_6$/C$_6$F$_6$ (1:1)]: δ −83.0 (m, 27F),

−117.5 (m, 18F), −123.3 (m, 36F), −124.4 (m, 18F), −127.8 (m, 18F).

1(1, 2, 8, C4): Anal. Calcd. for C$_{39}$H$_{25}$F$_{34}$PSi: C 39.08, H 2.10, P 2.58, F 53.89. Found: C 39.11, H 2.17, P 2.51, F 54.04.

1(2, 1, 8, C4): Anal. Calcd. For C$_{42}$H$_{33}$F$_{34}$PSi$_2$: C 39.70, H 2.62, P 2.44, F 50.83. Found: C 39.88, H 2.52, P 2.49, F 50.97.

1(3, 1, 10, C4): Anal. Calcd for C$_{60}$H$_{42}$F$_{62}$PSi$_3$: C 34.73, H 2.04, F 57.68, P 1.49. Found: C 35.06, H 2.15, F 57.63, P 1.49.

General Experimental Procedure for 1(a, b, x, C3C5). To a solution of **4**(a, C3C5) in THF (a = 3) or Et$_2$O (a = 2) was added a solution of t-BuLi in pentane (4.6a equiv) at − 90 °C. After the mixture had been stirred for 30 min, a solution of **3**(b, x) (4a equiv) in Et$_2$O was added, and the reaction mixture was warmed to room temperature. After

15 h, all solvent was removed in vacuo, and the residue was dissolved in CH_2Cl_2/degassed water [**1**(3, 1, *x*, C3C5); *x* = 4, 6] or FC-72/MeOH. Phase separation and evaporation of all volatiles yielded **1**(*a*, *b*, *x*, C3C5) as yellow to brown oils. For yields and ^{1}H and ^{31}P NMR data, see Table 7.

1(3, 1, 4, C3C5): Anal. Calcd. for $C_{66}H_{69}F_{54}PSi_6$: C 37.97, H 3.33, P 1.48, F 49.14. Found: C 38.20, H 3.26, P 1.53, F 48.92.

1(3, 1, 10, C3C5): Anal. Calcd. for $C_{102}H_{69}F_{126}PSi_6$: C 31.51, H 1.79, P 0.80, F 61.57. Found: C 31.62, H 2.11, P 0.78, F 61.45.

1(3, 2, 6, C3C5): Anal. Calcd. For $C_{120}H_{78}F_{156}PSi_6$: C 30.79, H 1.62, F 63.33, P 0.66. Found: C 30.66, H 1.78, F 63.40, P 0.64.

Determination of Partition Coefficients. A known amount of **1**(*a*, *b*, *x*, *pos*) (between 1 and 15 μmol) was dissolved in PFMCH (2.000 $\pm$ 0.002 mL) and toluene (2.000 $\pm$ 0.002 mL). The mixture was stirred and subsequently equilibrated at 0 °C. If not all of the solute was dissolved, the amount of solute was decreased.[15] When two clear layers were obtained, an aliquot (500 μL) from each layer was taken by syringe and evaporated to dryness by keeping the residue under vacuum (0.1 mbar) for 15 h (constant weight within 1 mg). Subsequently, the weight of the residue was determined. At higher partition coefficients, when gravimetric determination of the partition coefficient became too inaccurate, the partition coefficient was calculated from the amounts of phosphorus found in each phase by ICP-AAS analysis.

Fluorous Biphasic Hydrosilylation Catalyzed by [RhCl-(L)₃] [L = 1(3, 1, 8, C3C5)]. To a solution of **1**(3, 1, 8, C3C5) (365 mg, 111 μmol) in PFMCH was added a solution of [RhCl(COE)₂]₂ (13.3 mg, 18.5 μmol) in CH_2Cl_2. After the mixture had been stirred vigorously for 1 h, the organic layer was completely decolorized. The two phases were separated, and the fluorous phase was dried in vacuo, affording a red oil, which was not further analyzed. The red oil was dissolved in PFMCH (4 mL), and 1-hexene (9.4 mL, 74 mmol) and HSiMe₂Ph (5.7 mL, 37 mmol) were added.

The reaction mixture was heated to reflux, at which point a homogeneous solvent system was formed. After 15 min, the reaction mixture was analyzed by ^{1}H NMR spectroscopy and GC, and subsequently, it was cooled to room temperature. The phases were separated, and a new cycle was started. Leaching of the catalyst and free fluorous ligand was determined by Rh and P ICP-AAS analyses of an aliquot of the organic layer of the first cycle.

References and Notes

(1) (a) de Wolf, E.; van Koten, G.; Deelman, B.-J. *Chem. Soc. Rev.* **1999**, *28*, 37. (b) Horváth, I. T. *Acc. Chem. Res.* **1998**, *31*, 641. (c) Curran, D. P. *Angew. Chem., Int. Ed. Engl.* **1998**, *37*, 1174. (d) Cornils, B. *Angew. Chem., Int. Ed. Engl.* **1997**, *36*, 2057. (e) Hope, E. G.; Stuart, A. M. *J. Fluorine Chem.* **1999**, *100*, 75.

(2) (a) Alvey, L. J.; Rutherford, D.; Juliette, J. J. J.; Gladysz, J. A. *Organometallics* **1998**, *63*, 6302. (b) Bhattacharyya, P.; Gudmunsen, D.; Hope, E. G.; Kemmitt, R. D. W.; Paige, D. R.; Stuart, A. M. *J. Chem. Soc., Perkin Trans. 1* **1997**, 3609. (c) Hope, E. G.; Kemmitt, R. D. W.; Paige, D. R.; Stuart, A. M.; Wood, D. R. W. *Polyhedron* **1999**, *18*, 2913. (d) Bhattacharyya, P.; Croxtall, B.; Fawcett, J.; Fawcett, J.; Gudmunsen, D.; Hope, E. G.; Kemmitt, R. D. W.; Paige, D. R.; Russell, D. R.; Stuart, A. M.; Wood, D. R. W. *J. Fluorine Chem.* **2000**, *101*, 247.

(3) (a) Horváth, I. T.; Rábai, J. *Science* **1994**, *266*, 72. (b) Horváth, I. T.; Kiss, G.; Cook, R. A.; Bond, J. E.; Stevens, P. A.; Rábai, J.; Mozeleski, E. J. *J. Am. Chem. Soc.* **1998**, *120*, 3133. (c) Juliette, J. J. J.; Rutherford, D.; Horváth, I. T.; Gladysz, J. A. *J. Am. Chem. Soc.* **1999**, *121*, 2696. (d) Rutherford, D.; Juliette, J. J. J.; Rocaboy, C.; Horváth, I. T.; Gladysz, J. A. *Catal. Today* **1998**, *42*, 381. (e) Dinh, L. V.; Gladysz, J. A. *Tetrahedron Lett.* **1999**, *40*, 8995.

(4) (a) Hope, E. G.; Kemmitt, R. D. W.; Paige, D. R.; Stuart, A. M. *J. Fluorine Chem.* **1999**, *99*, 197. (b) Betzemeier, B.; Knochel, P. *Angew. Chem., Int. Ed. Engl.* **1997**, *36*, 2623. (c) Grigg, R.; York, M. *Tetrahedron Lett.* **2000**, *41*, 7255. (d) Schneider, S.; Bannwarth, W. *Helv. Chim. Acta* **2001**, *84*, 735. (e) Kainz, S.; Koch, D.; Baumann, W.; Leitner, W. *Angew. Chem., Int. Ed. Engl.* **1997**, *36*, 1628. (f) Koch, D.; Leitner, W. *J. Am. Chem. Soc.* **1998**, *120*, 13398. (g) Zhang, Q.; Luo, Z.; Curran, D. P. *J. Org. Chem.* **2000**, *65*, 8866.

(5) (a) Richter, B.; de Wolf, E.; Deelman, B.-J.; van Koten, G. PCT Int. Appl. WO 0018444, 2000. (b) Richter, B.; van Koten, G.; Deelman, B.-J. *J. Mol. Catal. A: Chem.* **1999**, *145*, 317. (c) Richter, B.; Spek, A. L.; van Koten, G.; Deelman, B.-J. *J. Am. Chem. Soc.* **2000**, *122*, 3945.

(6) (a) Kiss, L. E.; Kövesdi, I.; Rábai, J. *J. Fluorine Chem.* **2001**, *108*, 95. (b) Huque, F. T. T.; Jones, K.; Saunders, R. A.; Platts, J. A. *J. Fluorine Chem.* **2002**, *115*, 119.

(7) A universal thermodynamic model for the prediction of log *P* values of solutes in fluorous biphasic solvent systems was developed by employing the MOD theory: de Wolf, E.; Ruelle, P.; van den Broeke, J.; Deelman, B. J.; van Koten, G. *J. Phys. Chem. B* **2004**, *108*, 1458.

(8) Richter, B.; de Wolf, E.; van Koten, G.; Deelman, B.-J. *J. Org. Chem.* **2000**, *65*, 3885.

(9) de Wolf, E.; Speets, E. A.; Deelman, B.-J.; van Koten, G. *Organometallics* **2001**, *20*, 3686.

(10) Studer, A.; Jeger, P.; Wipf, P. Curran, D. P. *J. Org. Chem.* **1997**, *62*, 2917.

(11) Ravindar, V.; Hemling, H.; Schumann, H.; Blum, J. *Synth. Commun.* **1992**, *22*, 841.

(12) de Wolf, E.; Richter, B.; Deelman, B.-J.; van Koten, G. *J. Org. Chem.* **2000**, *65*, 5424.

(13) After the mixture had been stirred for 3 days, the organic layer was still not decolorized, despite the 3:1 P/Rh ratio. The incomplete reaction in the case of [RhCl(COD)]₂ is probably caused by a different mechanism of formation of [RhCl(L)₃]. It was reported that the first step starting from [RhCl(COD)]₂ is the breaking of the μ-chloride bridge, whereas substitution of COE is the first step using [RhCl-(COE)₂]₂, which probably occurs more easily for bulkier phosphines. See: Vijay, S. R.; Varshney, A.; Gray, G. M. *J. Organomet. Chem.* **1990**, *391*, 259.

(14) Montgomery, D. C. *Design and Analysis of Experiments*, 4th ed.; John Wiley and Sons: New York, 1997.

(15) Barthel-Rosa, L. P.; Gladysz, J. A. *Coord. Chem. Rev.* **1999**, *190−192*, 587.